Radiology

Christiane K. Kuhl, MD
Hans H. Schild, MD
Nuschin Morakkabati, MD

Published online
10.1148/radiol.2363040811
Radiology 2005; 236:789–800

Abbreviations:
BI-RADS = Breast Imaging Reporting and Data System
2D = two-dimensional

[1] From the Department of Radiology, University of Bonn, Sigmund-Freud-Str 25, D-53105 Bonn, Germany. Received May 4, 2004; revision requested July 19; revision received November 4; accepted December 14. **Address correspondence to** C.K.K. (e-mail: *kuhl@uni-bonn.de*).

Authors state no financial relationship to disclose.

Author contributions:
Guarantor of integrity of entire study, C.K.K.; study concepts and design, C.K.K., H.H.S.; literature research, C.K.K., N.M.; clinical studies, C.K.K., N.M.; data acquisition, C.K.K., N.M.; data analysis/interpretation, C.K.K.; statistical analysis, C.K.K.; manuscript preparation, C.K.K.; manuscript definition of intellectual content, C.K.K., H.H.S.; manuscript editing, C.K.K.; manuscript revision/review, C.K.K., H.H.S.; manuscript final version approval, all authors

Dynamic Bilateral Contrast-enhanced MR Imaging of the Breast: Trade-off between Spatial and Temporal Resolution[1]

PURPOSE: To investigate prospectively the trade-off between temporal and spatial resolution in dynamic contrast material–enhanced bilateral magnetic resonance (MR) imaging of the breast.

MATERIALS AND METHODS: Informed consent and institutional review board approval were obtained. An intraindividual comparative study was performed in 30 patients (mean age, 53 years; age range, 27–70 years) with a total of 54 enhancing lesions (28 benign and 26 malignant) who underwent dynamic MR imaging of the breast twice, once with a standard dynamic protocol (256 × 256 matrix, 69 seconds per acquisition) and once on a separate day with a modified dynamic protocol (400 × 512 matrix, 116 seconds per acquisition). Systematic qualitative analysis of morphologic features and region-of-interest–based analysis of enhancement kinetics were performed.

RESULTS: A statistically significant difference (generalized linear modeling) in enhancement rates of benign versus malignant lesions was lost when moving from the standard to the modified dynamic protocol. Kinetic information on signal intensity time course patterns was preserved. Delineation of lesion margins and internal architecture was clearly superior with the modified dynamic protocol, which allowed identification of lesion features associated with high positive predictive value or high negative predictive value for breast cancer. Ten benign lesions classified as Breast Imaging Reporting and Data System (BI-RADS) category 3 with the standard protocol were correctly downgraded to BI-RADS category 2 with the modified protocol owing to visualization of internal septations. Thirteen malignant lesions categorized as BI-RADS category 3 or 4 with the standard protocol were correctly upgraded to BI-RADS category 4 or 5 with the modified protocol owing to visualization of spicules or rim enhancement. Receiver operating characteristic analysis revealed a significantly larger area under the curve for results obtained with the modified dynamic protocol.

CONCLUSION: Increased spatial resolution significantly improves diagnostic confidence and accuracy at dynamic MR imaging, even if this improvement occurs at the expense of temporal resolution. Loss of kinetic information regarding enhancement rates proved to be not diagnostically relevant because enhancement rates showed broad overlap between benign and malignant lesions and were therefore of only limited diagnostic use in the individual patient. Kinetic information regarding time course pattern was preserved and confirmed as having high specificity and high positive predictive value.

There is broad agreement that, for magnetic resonance (MR) imaging of the breast, criteria related to the morphologic features and enhancement kinetics of a lesion should be evaluated (1–8). For a detailed analysis of lesion margins and internal architecture, as well

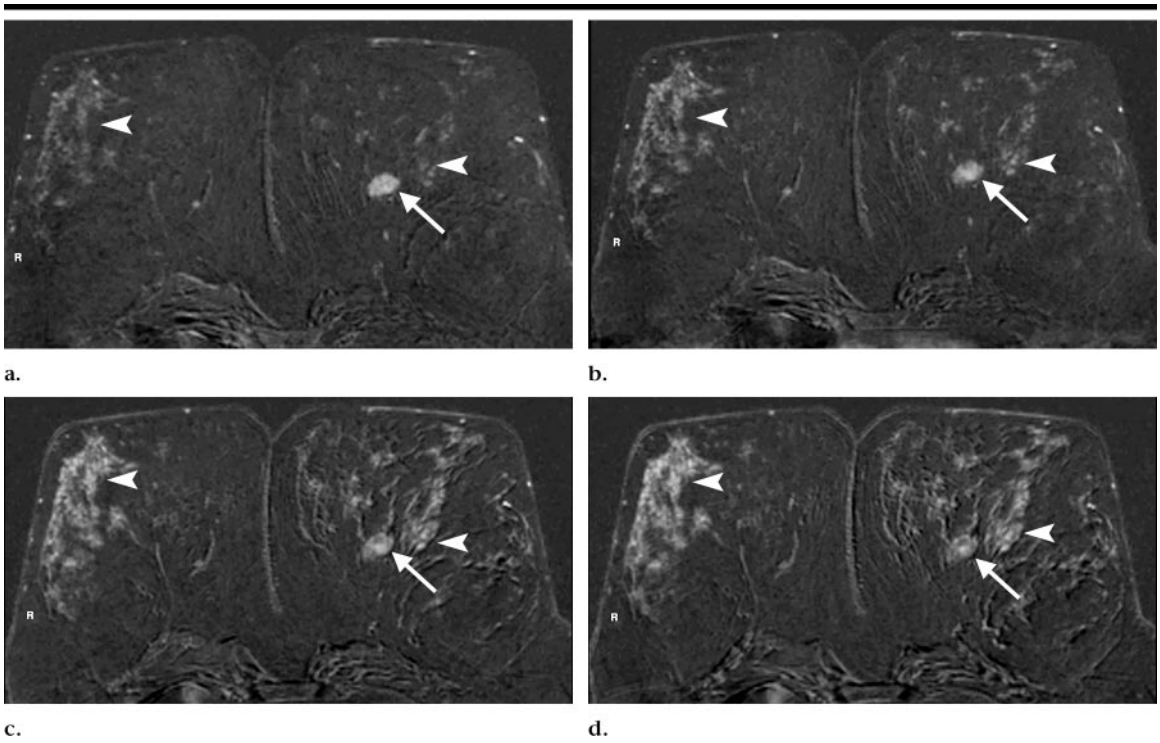

Figure 1. Transverse postcontrast dynamic subtracted MR images (270/4.6 [repetition time msec/echo time msec] and 90° flip angle) obtained at standard two-dimensional (2D) gradient-echo dynamic MR imaging (temporal resolution, 69 seconds per dynamic acquisition; imaging matrix, 256 × 256) of 53-year-old woman with invasive ductal cancer. Same section is displayed throughout dynamic series at **(a)** 69 seconds, **(b)** 2 minutes 18 seconds, **(c)** 3 minutes 27 seconds, and **(d)** 4 minutes 36 seconds after contrast material injection. Note that contrast between cancer (arrow) and normal fibroglandular tissue on both sides (arrowheads) is best in early postcontrast phase (**a**). Owing to strong washout effect in the cancer and progressive increase in signal intensity of normal parenchyma, cancer can be overlooked already on third postcontrast image (**c**). Assessment of fine morphologic details will not be feasible in these delayed postcontrast images because of lack of contrast between cancer and normal tissue.

as for the evaluation of kinetic features, a pulse sequence must be used that has a high spatial and high temporal resolution and covers the entire fibroglandular tissue. Temporal resolution (ie, acquisition speed) is required not only for assessment of the enhancement kinetics of a lesion during dynamic imaging but also because only in the early postcontrast phase is the lesion-to-parenchyma contrast such that an analysis of subtle morphologic features is feasible (Fig 1). Unfortunately, with currently available equipment, temporal and spatial resolution are competing demands, and any given pulse sequence will always be a compromise between these two divergent necessities. Therefore, while there is virtually universal agreement that adequate temporal and spatial resolution are important, little is known of what exactly constitutes "adequate" and where the compromise between spatial and temporal resolution should be set.

The purpose of this study was to investigate prospectively the trade-off between temporal and spatial resolution in dynamic postcontrast bilateral MR imaging of the breast. Standard dynamic bilateral MR imaging of the breast is usually performed with a temporal resolution of about 60 seconds per dynamic acquisition (3,9–13) and a 256 × 256 imaging matrix. Our aim was to find out whether it is useful to trade some of the temporal resolution for an increase of spatial resolution.

MATERIALS AND METHODS

Study Design and Inclusion Criteria

A prospective, comparative intraindividual study was performed in 30 women with 54 focal contrast material–enhancing lesions who underwent contrast-enhanced MR imaging of the breast twice, once with the standard dynamic protocol, which has been used for dynamic MR imaging of the breast for several years (1,3,9,12,13), and once with a modified dynamic protocol, for which some of the temporal resolution was traded for spatial resolution. Patients underwent diagnostic MR imaging for preoperative staging (n = 9), for follow-up after breast-conservation therapy (n = 4), for screening because of a high genetic risk of breast cancer (n = 8), or for clarification of inconclusive clinical or conventional imaging findings (n = 9). Patients were randomized to start with either the standard or the modified dynamic protocol during their first visit. To exclude any time-dependent changes or hormonal influences on contrast enhancement, all patients underwent the second MR imaging examination within 5 days after the first visit. In premenopausal women, care was taken to have the patient reinvestigated during the same week of the menstrual cycle. Patients gave written informed consent to participate after the experimental character of the study had been fully explained to them. The study design was approved by the authors' institutional review board. The mean age of the 30 participants was 53 years (age range, 27–70 years).

Diagnosis Validation

Diagnoses were validated by means of excisional biopsy or core biopsy in 34 of 54 focal breast lesions (26 breast cancer foci, two radial scars, four fibroadenomas, and two intramammary lymph nodes) and by means of clinical, mammographic, and MR imaging follow-up for at least 36 months in the remaining 20 lesions. It should be noted that resection of the four fibroadenomas was performed at the patients' request (ie, in spite of a final breast imaging diagnosis of Breast Imaging Reporting and Data System [BI-RADS] category 2 fibroadenoma). Among the 34 lesions with findings that were clarified at biopsy, 13 were visible at MR imaging alone. In these cases, MR-guided hook-wire placement and excisional biopsy (11 of 13 lesions) or MR-guided large core biopsy (two of 13 lesions) was performed. Although histologic findings were conclusive (fibroadenoma), the latter two patients underwent additional follow-up for 24 months to confirm the diagnosis of a benign lesion after MR-guided core biopsy.

MR Imaging of the Breast

At both visits, MR imaging was performed with a 1.5-T system (ACS II and ACS-NT; Philips Medical Systems, Best, the Netherlands) by using a standard bilateral breast coil. The protocol consisted of a T2-weighted turbo spin-echo sequence with a 280–320-mm field of view, 31 sections acquired, 3-mm section thickness, no intersection gap, 3800/120, turbo factor of 19, two signals acquired, and 512 × 512 matrix. This sequence was followed by the dynamic postcontrast series (standard dynamic protocol or modified dynamic protocol).

The standard dynamic protocol and modified dynamic protocol consisted of the same type of pulse sequence (2D gradient-echo sequence with linear phase-encode ordering), virtually identical contrast-determining parameters (270/4.6 and 90° flip angle [standard dynamic protocol] and 290/4.6 and 90° flip angle [modified dynamic protocol]), 29 sections acquired, 3-mm section thickness, no intersection gap, and an identical bilateral field of view (280–320 mm). For each sequence, 0.1 mmol per kilogram body weight gadopentetate dimeglumine (Magnevist; Schering, Berlin, Germany) was injected at a rate of 3 mL/sec by using a power injector (Solaris; Medrad, Indianola, Pa), which was followed by a 20-mL full saline flush. Sequences were performed with different acquisition matrices and, accordingly, with different acquisition times.

The standard dynamic protocol has been described previously (3). It consisted of seven dynamic image stacks: one acquired prior to the injection of contrast material and the remaining six acquired directly after the injection of contrast material. Dynamic acquisition was achieved with a full 256 × 256 matrix, an in-plane resolution of 1.25 × 1.25 mm for a 320-mm field of view, and a temporal resolution of 69 seconds.

For the modified dynamic protocol, the acquisition matrix was increased to 400 × 512, resulting in an in-plane pixel size of 0.80 × 0.60 mm. With this parameter setup, the acquisition time (ie, temporal resolution) was 116 seconds. Because of the longer acquisition time, only five image stacks (one precontrast and four postcontrast images) were acquired.

The respective dynamic series of the standard and modified dynamic protocols were transferred to a workstation (Easyvision; Philips Medical Systems). Image subtraction was performed by subtracting the precontrast images from all postcontrast images.

Enhancement Kinetics

Enhancing lesions were identified on subtracted images and were further evaluated by using a region-of-interest–based analysis as described previously (3). In short, manually drawn regions of interest were positioned by one of the authors (N.M., 6 years experience in MR imaging of the breast). These regions of interest were selectively placed into the area of the lesion where the enhancement was strongest in the first nonsubtracted postcontrast image. Care was taken to avoid nonenhancing or slowly enhancing lesion areas. Region of interest diameter was adjusted to the respective lesion diameter, with a mean region of interest diameter of 5 mm (range, 2–10 mm). Lesion signal intensity was plotted versus time to yield the signal intensity time course.

Lesion enhancement rates (ie, wash-in rates) were calculated according to the formula $[(SI_c - SI)/SI] \cdot 100$, where SI is the signal intensity of the lesion in the precontrast image and SI_c is the signal intensity of the lesion in the first postcontrast image. Enhancement rates were calculated for the first (ER1) and second (ER2) postcontrast acquisition obtained with the standard dynamic protocol (ie, the first and second postcontrast minute) and for the first postcontrast acquisition obtained with the modified dynamic protocol (ER) (because of the lower temporal resolution, there was no 1st minute enhancement value available for the modified dynamic protocol). Enhancement rates of benign and malignant lesions in the first and second postcontrast acquisition of the standard dynamic protocol (ER1 and ER2) were compared with the enhancement rates of the same lesions in the first postcontrast acquisition of the modified dynamic protocol (ER).

We analyzed both ER1 and ER2 of the standard dynamic protocol in order to investigate whether there were differences regarding the differential diagnostic potency of the criterion "enhancement rate" with a more rapid acquisition (ER1) compared with a slower acquisition (ER2), which corresponded to higher spatial resolution.

As described previously (3), the cutoff, or threshold, value for lesion enhancement was calculated by subtracting the respective single standard deviation from the mean enhancement rate of breast cancers in the study population. The sensitivity and specificity of ER1 and ER2 of the standard dynamic protocol and that of the modified dynamic protocol were calculated by determining the number of benign lesions that demonstrated an enhancement rate above the threshold value and by determining the number of malignant lesions that demonstrated an enhancement rate below the threshold value.

Two breast radiologists (N.M. and C.K.K., with 6 and 12 years of experience in dynamic MR imaging of the breast, respectively) were presented signal intensity time courses for the enhancing lesions (108 time courses for 54 lesions in two different protocols). Readers were blinded to the corresponding lesion morphologic features (ie, readers were presented the time courses alone, without the MR image of the respective lesion) and were asked to classify, in consensus, the signal intensity time course of the lesions according to one of three types (3). A type 1 (persistent enhancement) time course was assigned if the signal intensity increased steadily throughout the dynamic period. A type 2 (plateau) time course was assigned if peak signal intensity was reached in the early postcontrast period and was followed by a plateau of signal intensity in the remaining dynamic series. A type 3 (washout) time course was assigned if peak signal intensity was reached in the early phase and was immediately followed by a loss of

signal intensity in the early postcontrast period.

Assessment of Morphologic Features

Two breast radiologists (N.M., C.K.K.) who were blinded to lesion enhancement kinetics (ie, wash-in rates and time course patterns) were asked to classify, in consensus, the lesion shape (round, ovoid, irregular, or stellate), margins (smooth, non-smooth, or spicules), and internal architecture (homogeneous, heterogeneous, rim enhancement, or low-signal-intensity internal septations) of the enhancing lesions. Early postcontrast subtracted images and precontrast and early postcontrast nonsubtracted images were made available. To avoid biased decisions, images were displayed in randomized order for each protocol.

Clinical Image Interpretation

Two breast radiologists (N.M., C.K.K.) who were blinded to the respective clinical history and to the mammographic or ultrasonographic findings reviewed the MR images in consensus. Precontrast and early, intermediate, and late postcontrast images—including subtracted images of the early, intermediate, and late postcontrast phase—and the lesion signal intensity time course were made available. Just as in the regular clinical situation, nonsubtracted and subtracted images were transferred to hard-copy films by using standardized window settings. Image sets obtained with each of the different protocols were presented in a randomized order for each patient.

Readers were asked to mention the number of enhancing lesions detected on the hard-copy films; lesions were numbered consecutively to allow unambiguous identification. Readers were also asked to categorize the probability of malignancy for each lesion according to the BI-RADS classification (2,14).

The diagnostic criteria that were used to classify lesions were based on lesion morphologic features (shape, margins, and internal architecture) and lesion enhancement kinetics (enhancement rate in the early postcontrast phase and signal intensity time course pattern in the intermediate and late postcontrast phase) (12,15). A BI-RADS category 1 was assigned if there was no enhancement at all. A BI-RADS category 2 was assigned if the lesion shape and margins suggested a benign lesion and if the internal architecture demonstrated low-signal-intensity internal septations (fibrodenoma), irrespective of enhancement rates or time course kinetics. A BI-RADS category 2 was also assigned if the internal architecture was homogeneous or slightly heterogeneous and if the shape, margins, and time course kinetics suggested a benign lesion (slow enhancement rate and type 1 time course). A BI-RADS category 3 was assigned if the shape and margins were unsuspicious, enhancement rates were fast, and a type 1 or 2 time course was observed. A BI-RADS category 4 was assigned if, in the same setting, a type 3 (washout) time course was observed. A BI-RADS category 4 was also assigned in lesions with a suspicious shape and margin status but benign-appearing kinetics (slow enhancement rate and type 1 time course). A BI-RADS category 5 was assigned if both the morphologic features and the time course kinetics indicated a malignant lesion. A BI-RADS category 5 was also assigned as soon as rim enhancement was noted, irrespective of shape, margins, enhancement rates, and time course kinetics. In such cases, however, the corresponding T2-weighted turbo spin-echo and precontrast T1-weighted images were made available to exclude a cyst with inflammatory changes or a region of fat necrosis as the reason for rim enhancement.

TABLE 1
Distribution according to Lesion Type for 54 Lesions in 30 Patients

Lesion Type	No. of Patients	No. of Lesions
Benign (n = 28)		
Fibroadenoma	11	24
Lymph node hyperplasia	2	2
Radial scar	2	2
Malignant (n = 26)		
Ductal carcinoma in situ	1	1
Invasive cancer	14	25
Total	30*	54

* One patient had both a malignant lesion and an intramammary lymph node.

Statistical Analysis

For statistical analysis, a commercially available software package (Excel 2000; Microsoft, Redmond, Wash) was used. Mean values, ranges, and standard deviations were calculated for quantitative parameters (enhancement rates of focal enhancing lesions and signal-to-noise ratios). For the standard dynamic protocol, a t test for matched pairs was performed to compare enhancement rates of benign and malignant lesions between the first and second postcontrast images.

To calculate sensitivity and specificity of diagnoses made on the basis of the standard and corresponding modified dynamic images, diagnoses were dichotomized; BI-RADS categories 1–3 were classified as benign, and BI-RADS categories 4 and 5 were classified as malignant. The histologic diagnoses and results of 2-year follow-up served as a standard of reference. For this purpose, invasive or intraductal cancers were categorized as malignant whereas other lesions, including radial scars, were categorized as benign. A Wilcoxon matched pairs signed rank test was performed to test for statistical significance regarding the assignment of time course patterns and BI-RADS diagnoses in the same lesions for modified and standard dynamic protocols. Enhancement rates of benign versus malignant lesions were also compared for both protocols.

To account for the correlation between multiple lesions in the same patient, generalized linear modeling and generalized estimation equations were used for the estimation of mean enhancement rates and confidence limits. For both dynamic protocols, receiver operating characteristic analyses of the final BI-RADS categories were performed for each respective lesion and were compared by using the technique described by DeLong et al (16). A P value of less than .05 was considered to indicate a statistically significant difference.

RESULTS

A total of 54 contrast-enhanced lesions were identified in 30 patients (Table 1). Fifteen patients had a total of 28 benign lesions. Of these patients, two had a radial scar, 11 had 24 fibroadenomas, and two had an intramammary lymph node. In the remaining 15 patients, 26 malignant lesions were identified. One patient

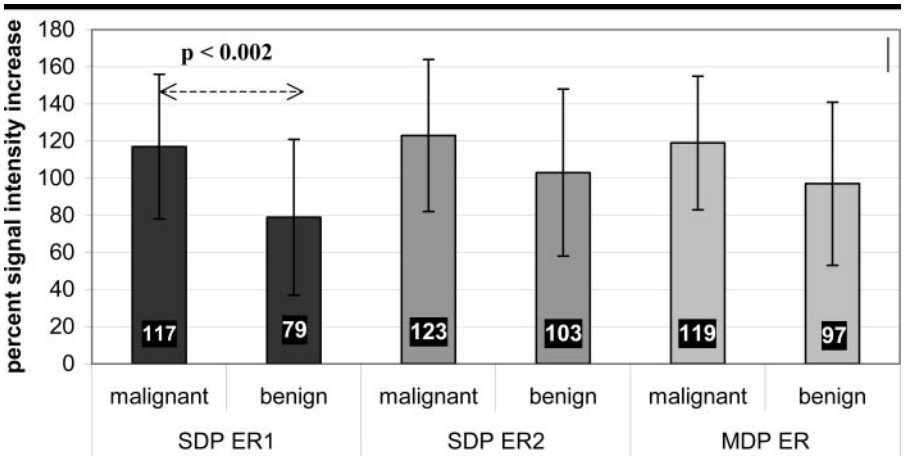

Figure 2. Graph demonstrates mean enhancement rates of benign ($n = 28$) and malignant ($n = 26$) breast lesions for standard dynamic protocol (*SPD*) and modified dynamic protocol (*MDP*). Values are given for first postcontrast dynamic image (*ER1*) obtained 69 seconds after contrast material injection and second postcontrast dynamic image (*ER2*) obtained 138 seconds after contrast material injection for standard dynamic protocol and for first postcontrast dynamic image (*ER*) obtained 116 seconds after contrast material injection for modified dynamic protocol. Respective values of mean enhancement rates are given on bottom of bars. Note that a significant difference in mean enhancement rates between benign and malignant lesions was present only in ER1.

had both a breast cancer in one breast and a hyperplastic intramammary lymph node in the contralateral breast. The mean diameter of benign, enhancing breast lesions was 8 mm (standard deviation, 4 mm; range, 3–17 mm), and the mean diameter of malignant, enhancing lesions was 10 mm (standard deviation, 9 mm; range, 3–46 mm).

Enhancement Rates

An overview of the mean enhancement rates of benign and malignant lesions for both dynamic protocols is given in Figure 2. For the standard dynamic protocol, values for both the first (ER1, 69 seconds after contrast material injection) and second (ER2, 116 seconds after contrast material injection) dynamic postcontrast images are given.

For the standard dynamic protocol, the difference between the enhancement rates of benign and malignant lesions in the first dynamic postcontrast images (ER1, 69 seconds after contrast material injection) was 34.8% (95% confidence interval: 0.186, 0.510; $P < .001$). This difference was smaller (16.6%) in the second postcontrast image (ER2) obtained 138 seconds after contrast material injection (95% confidence interval: −0.025, 0.356; $P > .05$). The loss of a statistically significant difference in the enhancement rates of benign versus malignant lesions that occurred in the second postcontrast acquisition resulted from the fact that benign lesions exhibited a significant increase in signal intensity between the first and second dynamic acquisitions ($P < .001$), whereas the signal intensity of malignant lesions remained about the same ($P > .2$). The second postcontrast image obtained with the standard dynamic protocol (ER2) and the first postcontrast image obtained with the modified dynamic protocol yielded comparable enhancement rates, and the difference between the enhancement rates of benign and malignant lesions (15.4%) was leveled out with the modified dynamic protocol just as it was during acquisition of the second postcontrast image for the standard dynamic protocol (95% confidence interval: −0.011, 0.319; $P > .05$).

The cutoff, or threshold, enhancement rate was calculated as 74% for the first postcontrast image obtained with the standard dynamic protocol and as 78% for the first postcontrast image obtained with the modified dynamic protocol. For the first postcontrast image obtained with the standard dynamic protocol (ER1, 69 seconds after contrast material injection), a total of 15 of 28 benign lesions demonstrated an enhancement rate above the threshold value, and four of 26 malignant lesions demonstrated an enhancement rate below the threshold value. For the first postcontrast image obtained with the modified dynamic protocol (116 seconds after contrast material injection), 20 of 28 benign lesions demonstrated enhancement above the threshold value, and four of 26 malignant lesions demonstrated enhancement below the threshold value.

To calculate the diagnostic accuracy of the enhancement rates, an enhancement rate above threshold was considered malignant and an enhancement rate below threshold was considered benign. For the standard dynamic protocol, the sensitivity, specificity, and positive predictive value of the criterion "enhancement rate" for the first postcontrast image (ER1) were 85% (22 of 26 lesions), 46% (13 of 28 lesions), and 60% (22 of 37 lesions), respectively. For the modified dynamic protocol, the sensitivity, specificity, and positive predictive value of the enhancement rate criterion were 85% (22 of 26 lesions), 29% (eight of 28 lesions), and 52% (22 of 42 lesions), respectively.

Analysis of Signal Intensity Time Course

The distribution of signal intensity time course patterns for the standard dynamic protocol and modified dynamic protocol is given in Figure 3. In 47 (87%) of 54 lesions, the same time course pattern was observed for both protocols. The distribution of time course patterns between these two protocols did not differ significantly (Wilcoxon matched pairs signed rank test).

Seven (13%) of 54 lesions had discordant classifications. Of these seven lesions, two were benign and five were malignant. In three of the five malignant lesions, a type 3 (washout) time course was demonstrated with the modified dynamic protocol whereas a type 2 (plateau) time course was demonstrated with the standard dynamic protocol (Fig 4). In the other two malignant lesions, a type 2 (plateau) time course was demonstrated with the modified dynamic protocol whereas a type 3 (washout) time course was demonstrated with the standard dynamic protocol. Discordant classifications were further observed in two of the 28 benign lesions. In one radial scar, the time course pattern was rated as type 1 (persistent enhancement) with the standard dynamic protocol whereas, with the modified dynamic protocol, the time course pattern was rated as type 2 (plateau). In one intramammary lymph node, a type 3 (washout) time course was demonstrated with the standard dynamic protocol whereas a type 2 (plateau) time course was demonstrated with the modified dynamic protocol.

To determine the sensitivity, specific-

ity, and positive predictive value of the criterion "time course patterns," a type 1 time course was considered indicative of a benign lesion and a type 2 or type 3 time course was considered indicative of a malignant lesion. This criterion had a sensitivity of 96% (25 of 26 lesions) for both protocols, a positive predictive value of 86% (25 of 29 lesions) and 83% (25 of 30 lesions) for the standard and modified dynamic protocol, respectively, and a specificity of 86% (24 of 28 lesions) and 82% (23 of 28 lesions) for the standard and modified dynamic protocol, respectively.

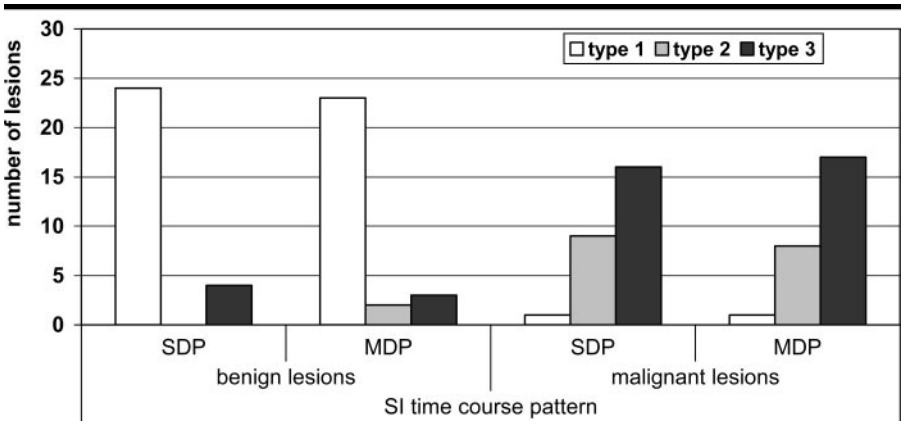

Figure 3. Graph demonstrates distribution of different signal intensity (*SI*) time course patterns in benign and malignant lesions for standard and modified dynamic protocols. Type 1 corresponds to a time course with a persistent, progressive increase in signal intensity throughout dynamic series, type 2 corresponds to a curve with plateau formation, and type 3 corresponds to a time course with early washout. *MDP* = modified dynamic protocol, *SPD* = standard dynamic protocol.

TABLE 2
Comparison of the Detectability of Key Lesion Features with Standard and Modified Dynamic Protocol

Lesion Features	Standard Dynamic Protocol	Modified Dynamic Protocol
Fibroadenomas (n = 21)		
Smooth borders	20/24 (83)	24/24 (100)
Internal septations	6/24 (25)	13/24 (54)
Invasive cancers and ductal carcinoma in situ (n = 24)		
Spicules	6/26 (23)	19/26 (73)
Rim enhancement	4/26 (15)	6/26 (23)

Note.—Numbers in parentheses are percentages.

Analysis of Morphologic Features

Regarding the delineation of anatomic details of lesion margins or internal architecture, the assessment of benign and malignant lesions with a standard versus modified dynamic protocol differed in 21 of 54 lesions, specifically in 13 of 26 malignant lesions and eight of 28 benign lesions. The detectability of key morphologic features is given in Table 2.

For the modified dynamic protocol and standard dynamic protocol, spicules were identified in 19 (73%) of 26 and six (23%) of 26 malignant lesions, respectively—that is, in 13 (50%) of 26 malignant lesions, spicules were identified with the modified dynamic protocol whereas only irregular borders or smooth borders were identified with the standard dynamic protocol (Fig 4). For the modified dynamic protocol and standard dynamic protocol, smooth borders were identified in 24 (100%) of 24 and 20 (83%) of 24 fibroadenomas, respectively—that is, in four (17%) of 24 fibroadenomas, smooth borders were demonstrated with the modified dynamic protocol whereas non-smooth margins were demonstrated with the standard dynamic protocol; this was probably the result of partial volume effects.

Regarding the analysis of internal architecture, the modified dynamic protocol allowed detection of rim enhancement in six (23%) of 26 malignant lesions, as opposed to the standard dynamic protocol, which allowed detection of rim enhancement in only four (15%) of 26 malignant lesions. In turn, the modified dynamic protocol allowed delineation of low-signal-intensity internal septations in 13 (54%) of 24 fibroadenomas (Fig 5), as opposed to the standard dynamic protocol, which allowed delineation of septations in only six (25%) of the same 24 fibroadenomas.

The modified dynamic protocol allowed identification of diagnostically relevant details regarding lesion margin or internal architecture in a total 26 (48%) of 54 lesions. In none of the patients were anatomic details identified with the standard dynamic protocol that were not identified with the modified dynamic protocol.

Clinical Image Interpretation

In the 30 patients, all 54 lesions were prospectively and independently diagnosed by using both dynamic protocols. The BI-RADS categories that were assigned with the standard and modified dynamic protocols are given in Table 3. Concordant BI-RADS categories were assigned in 30 (56%) of 54 lesions. Divergent BI-RADS categories were assigned in 24 of (44%) 54 lesions. The discrepant BI-RADS categories were observed as follows:

Benign lesions.—A total of seven fibroadenomas that received a BI-RADS category 3 with the standard dynamic protocol were classified as BI-RADS category 2 with the modified dynamic protocol because internal septations were visible (Fig 5). In a patient with contralateral breast cancer, one 6-mm intramammary lymph node that appeared round and well circumscribed with the standard dynamic protocol was categorized as BI-RADS category 3; however, because this lesion appeared kidney-shaped with central fatty tissue on precontrast images obtained with the modified dynamic protocol, it was categorized as BI-RADS category 2 (lymph node). Four fibroadenomas that appeared irregular with the standard dynamic protocol (BI-RADS category 3) were identified as having smooth margins with the modified dynamic protocol (BI-RADS category 2). One radial scar was categorized as BI-RADS category 4 with the standard dynamic protocol, whereas the same lesion was categorized as BI-

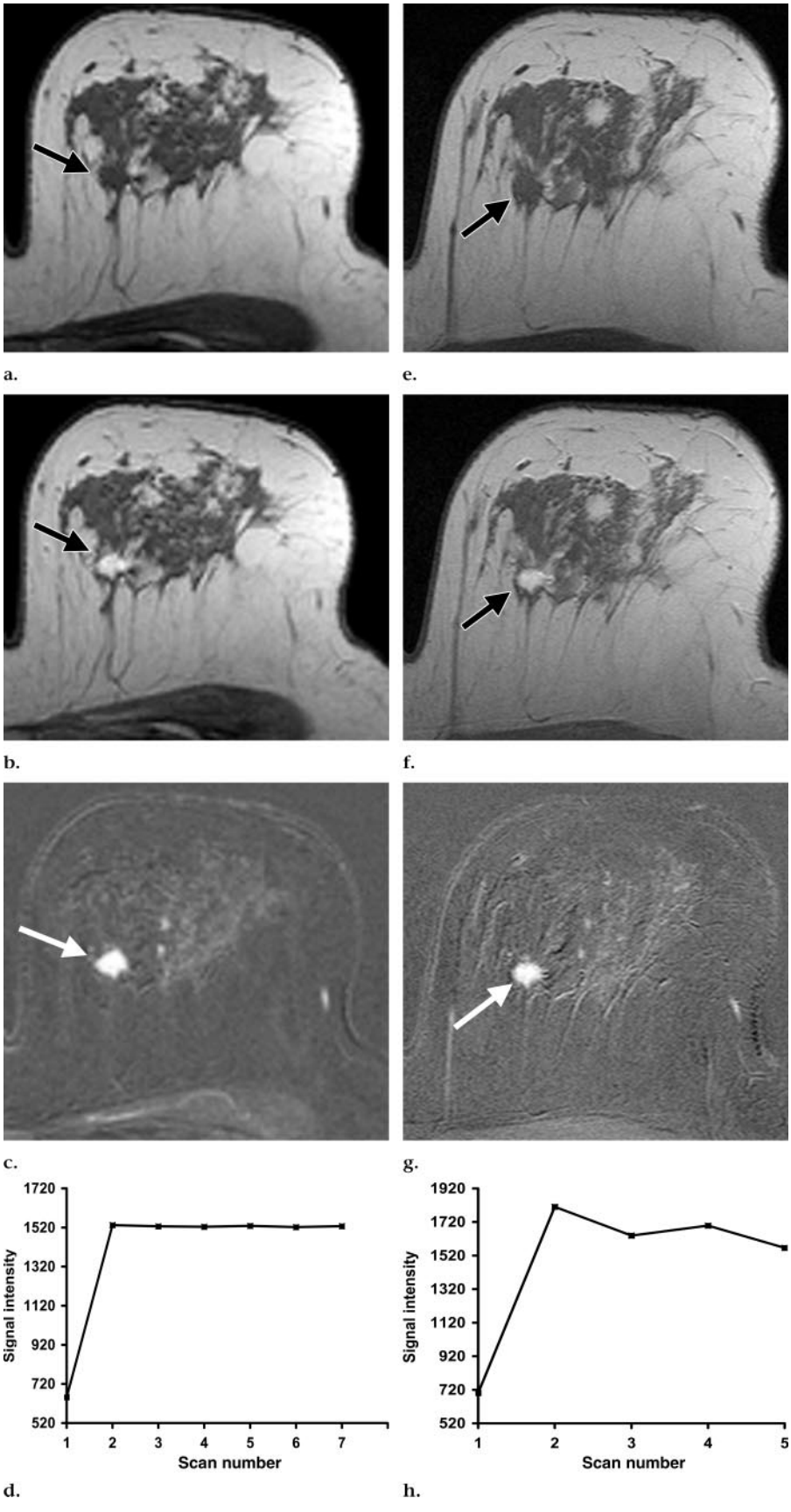

Figure 4. Transverse T1-weighted gradient-echo MR images (2D gradient-echo sequence, 290/4.6, and 90° flip angle) and corresponding signal intensity time course graphs for 62-year-old woman with breast cancer who underwent MR imaging for preoperative staging. **(a–c)** For standard dynamic protocol (256 × 256 imaging matrix with temporal resolution of 69 seconds), enhancing breast cancer (arrow in **a**, **b**, and **c**) appeared as irregular mass with smooth borders in **(a)** precontrast image, **(b)** first postcontrast image, and **(c)** first subtracted postcontrast image. **(d)** Graph demonstrates type 2 (plateau) signal intensity time course for standard dynamic protocol. Lesion was rated as BI-RADS category 4. **(e–g)** For modified dynamic protocol (400 × 512 imaging matrix with temporal resolution of 116 seconds), spicules were visualized at site of enhancing breast cancer (arrow in **e**, **f**, and **g**) in **(e)** precontrast image, **(f)** first postcontrast image, and **(g)** first subtracted postcontrast image (note the visible spicules). **(h)** Graph demonstrates type 3 (washout) signal intensity time course for modified dynamic protocol. Lesion was rated as BI-RADS category 5. Contrast enhancement kinetics were equivalent (strong early enhancement above threshold and plateau time course) for both protocols.

RADS category 5 with the modified dynamic protocol because spicules were visible. Thus, for benign lesions, the modified dynamic protocol allowed a correct BI-RADS downgrading of 10 (36%) of 28 benign lesions; in one (4%) of 28 lesions, the modified dynamic protocol resulted in false-positive BI-RADS upgrading of a benign lesion.

Malignant lesions.—Thirteen (50%) of 26 malignant lesions were correctly upgraded with the modified dynamic protocol compared with the standard dynamic protocol. In nine of 26 malignant lesions, a BI-RADS category 4 with the standard dynamic protocol was upgraded to a BI-RADS category 5 with the modified dynamic protocol owing to the visualization of spicules, rim enhancement, and/or a washout time course (Figs 4, 6). Four of 26 malignant lesions that were assigned a BI-RADS category 3 with the standard dynamic protocol were upgraded to a category 4 or 5 with the modified dynamic protocol (Fig 6). In no malignant lesion was the BI-RADS category assigned with the modified dynamic protocol lower than that assigned with the standard dynamic protocol. Thus, a false-negative downgrading of a lesion did not occur.

In 23 (43%) of 54 lesions (10 benign and 13 malignant), a more confident diagnosis was achieved with the modified dynamic protocol than was achieved with the standard dynamic protocol. In

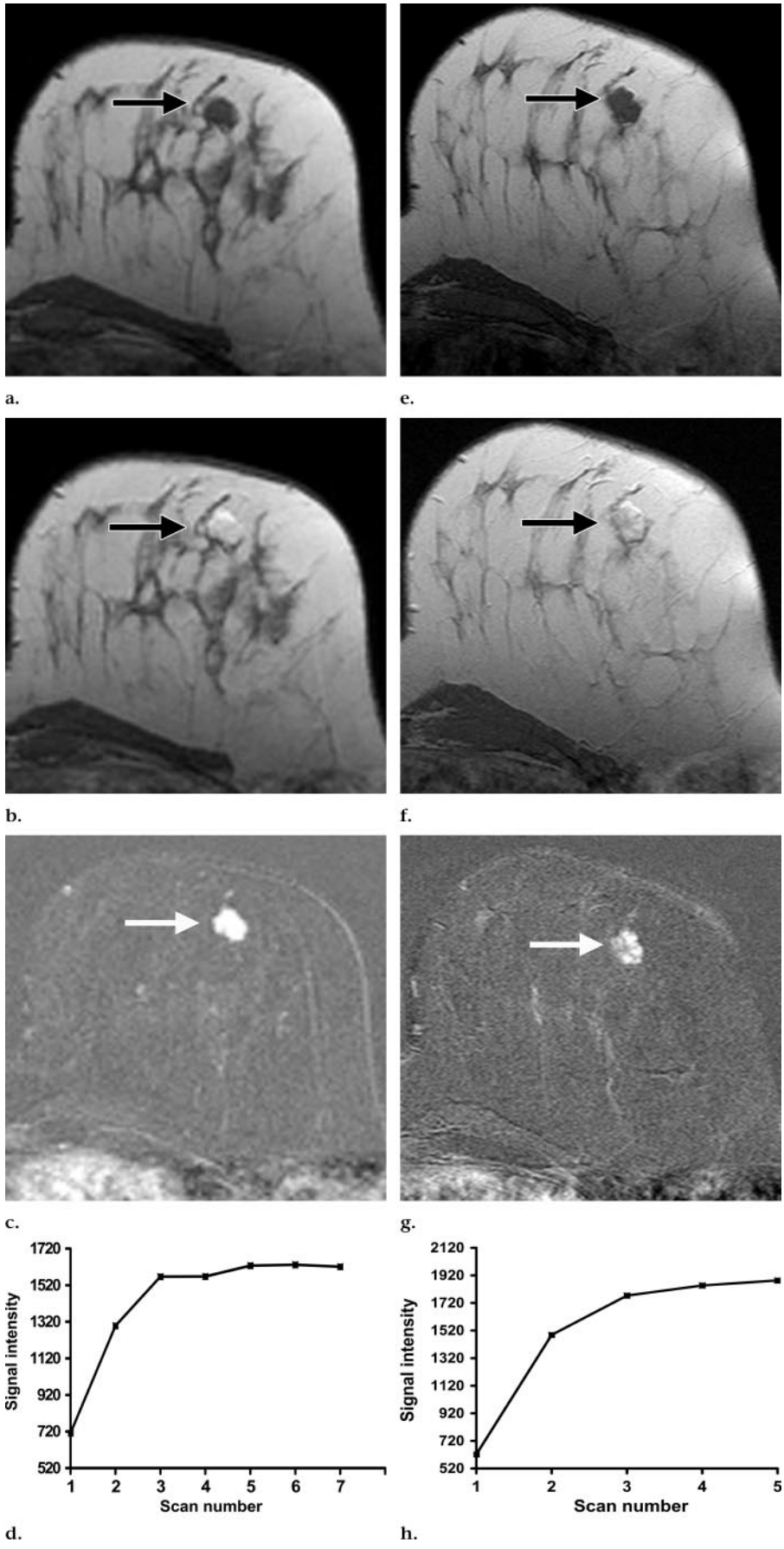

Figure 5. Transverse T1-weighted gradient-echo MR images (2D gradient-echo sequence, 290/4.6, and 90° flip angle) and corresponding time course graphs for 51-year-old woman with history of cancer in left breast who underwent follow-up MR imaging. Focal mass was present that exhibited oval shape and smooth borders. **(a–c)** For standard dynamic protocol (256 × 256 imaging matrix with temporal resolution of 69 seconds), internal enhancement seemed homogeneous. Arrow indicates site of lesion in **(a)** precontrast image, **(b)** first postcontrast image, and **(c)** subtraction of first postcontrast image (note the homogeneous internal enhancement of lesion). **(d)** Graph demonstrates type 1 (persistent enhancement) signal intensity time course of the enhancing lesion for standard dynamic protocol. Lesion was rated as BI-RADS category 3 (probably benign), and 6-month follow-up was recommended. **(e–g)** For modified dynamic protocol (512 × 400 imaging matrix with temporal resolution of 116 seconds), internal low-signal-intensity internal septations became visible. Lesion was categorized as BI-RADS category 2, and findings at long-term follow-up for 36 months confirmed presence of fibroadenoma. Arrow indicates site of lesion in **(e)** precontrast image, **(f)** first postcontrast image, and **(g)** subtraction of first postcontrast image. Note low-signal-intensity internal septations in **f** and **g**. **(h)** Graph demonstrates type 1 (persistent enhancement) signal intensity time course for modified dynamic protocol. Time course was equivalent to that seen in **d**.

none of the 54 lesions was a diagnosis established with higher confidence on the basis of standard dynamic images.

The receiver operating characteristic analysis revealed a statistically significant difference in the area under the receiver operating characteristic curve, which was larger for the modified dynamic protocol (0.945) than for the standard dynamic protocol (0.877) ($P < .05$).

DISCUSSION

Dynamic MR imaging is increasingly used in addition to conventional mammography and high frequency ultrasonography to improve the timely diagnosis of primary and recurrent breast cancer (12,15,17–29). While the high sensitivity of dynamic MR imaging is well established, its specificity remains an issue of debate. Many technical and interpretative approaches have been developed over the past years to help improve the differential diagnosis of enhancing lesions. There is agreement in that the specificity is improved if both morphologic and kinetic features are used for analysis (1,3,7,8). It has been shown that a washout time course can help diagnose

TABLE 3
Comparison of BI-RADS Categories Assigned to Benign and Malignant Lesions according to Standard and Modified Dynamic Protocol

Lesion Type and No.	Standard Dynamic Protocol	Modified Dynamic Protocol
Benign		
1	3	3
2	3	3
3	3	2
4	3	2
5	5	5
6	3	2
7	3	3
8	3	3
9	2	2
10	3	3
11	4	5
12	3	3
13	3	2
14	2	2
15	3	2
16	2	2
17	3	2
18	3	3
19	3	3
20	2	2
21	3	3
22	2	2
23	2	2
24	4	4
25	3	2
26	3	2
27	3	2
28	3	2
Malignant		
29	4	5
30	4	5
31	5	5
32	3	4
33	3	4
34	5	5
35	5	5
36	5	5
37	4	4
38	3	4
39	4	5
40	5	5
41	4	5
42	5	5
43	4	4
44	5	5
45	5	5
46	3	3
47	4	5
48	4	5
49	5	5
50	4	5
51	3	5
52	4	5
53	5	5
54	4	5

breast cancers that exhibit benign morphologic features (2,3,30); in turn, lesion architectural features are known to offer a high positive or high negative predictive value for breast cancer (4,6,7,31). Thus, while there is broad agreement that, for MR imaging of the breast, a pulse sequence should be used that compromises the demands of a high spatial and high temporal resolution, there are not enough data available that would substantiate how and where this compromise should be set. In other words, there is only little information available on the degree of temporal resolution that is actually needed to allow for the assessment of the most widely used kinetic features (ie, wash-in rates and time course patterns).

The standard protocol for dynamic bilateral MR imaging was proposed soon after the introduction of postcontrast MR imaging of the breast (3,9) and has changed little since then. Typically, 2D or three-dimensional gradient-echo techniques with a temporal resolution of about 69 seconds per dynamic acquisition and a spatial resolution of 256 × 256 for a bilateral field of view (usually 350 mm) are used. Fast acquisition strategies have been proposed in an attempt to further improve the kinetic analysis, including pharmacokinetic modeling, but these strategies have not gained broad clinical acceptance (32–36). This is because, first, these pulse sequences usually do not cover the entire breast parenchyma, and, second, these sequences sacrifice almost all morphologic information in favor of acquisition speed, thus precluding the combined analysis of morphologic features and kinetics. Also, it is unclear to date whether the additional kinetic data points and pharmacokinetic modeling of these sequences add diagnostically useful information compared with that provided by the standard dynamic protocol (31,37,36) and plain visual time course analysis (3).

On the other end of the spectrum, high-spatial-resolution techniques are commonly used for MR imaging of the breast, particularly in the United States (6,38,39). These techniques are not designed to provide a kinetic analysis and currently focus on imaging of a single breast, which limits the use of these techniques in many screening and staging settings. New acquisition strategies—for example, volume imaging for breast assessment, also known as VIBRANT, or parallel imaging techniques, such as sensitivity encoding, also known as SENSE (40)—may allow bilateral sagittal imaging in a kinetic mode, but these techniques are currently not available on a broader scale and still require validation before they can be recommended for clinical use.

A combination of dynamic acquisition and the delayed acquisition of high-spatial-resolution fat-suppressed images (three-dimensional spectral-spatial excitation magnetization transfer, also known as SSMT) 9 minutes after contrast material injection is another approach that has been proposed as a compromise (4). A possible disadvantage of this technique is the fact that breast cancers tend to demonstrate contrast material washout in the early postcontrast period (this occurred in 17 of 24 breast cancers in our study cohort). This loss of signal intensity, together with the progressive increase in signal enhancement of the adjacent fibroglandular tissue, may reduce or even cancel out the lesion-to-parenchyma contrast in the delayed postcontrast phase. The advantage of delayed high-spatial-resolution imaging may, therefore, be of only limited value, particularly in the assessment of malignant tissues.

Our objective was to explore whether it would be diagnostically useful to shift our current compromise between temporal and spatial resolution in dynamic bilateral MR imaging of the breast to improve the assessment of morphologic details. We sought to answer the following questions: First, compared with the temporal resolution of the standard dynamic protocol (256 × 256 imaging matrix with temporal resolution of 69 seconds per dynamic acquisition), is the loss of temporal resolution with a modified dynamic protocol (116 seconds vs 69 seconds per dynamic acquisition) diagnostically relevant? Specifically, does the reduced sampling rate secondary to the decreased temporal resolution impair the assessment of enhancement rates and time course patterns? And, if so, is this clinically important? Second, does the moderate increase in spatial resolution (from a 256 × 256 imaging matrix to a 400 × 512 imaging matrix) improve the assessment of lesion morphologic details to a degree that would be diagnostically relevant? Finally, is there a difference regarding the diagnostic accuracy and/or the diagnostic confidence with which enhancing lesions can be classified?

Regarding the first issue (ie, the effect of a reduced temporal resolution), our findings suggest that the modified dynamic protocol does in fact lead to a loss of kinetic information. At 69 seconds after contrast material injection (first postcontrast image, standard dynamic protocol), benign and malignant lesions demonstrated a significantly different enhancement rate, with malignant lesions showing a significantly higher wash-in rate compared with that of benign lesions. This difference was lost at 2 minutes after contrast material injection

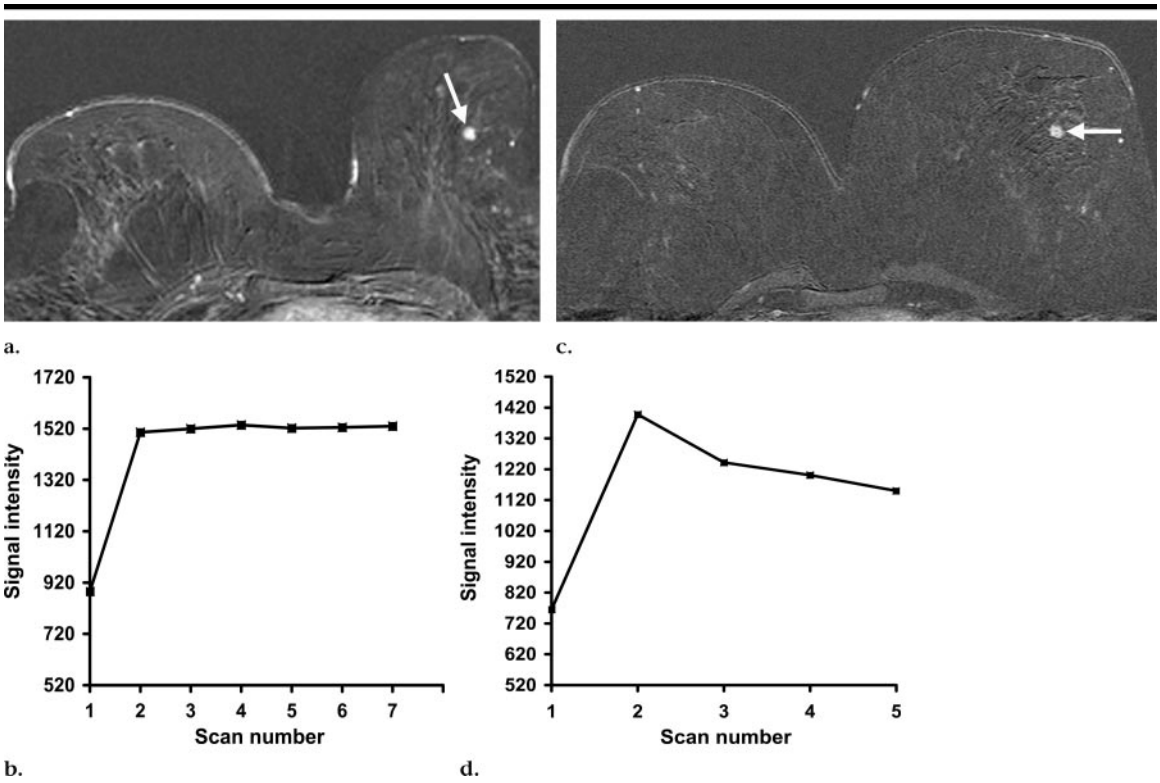

Figure 6. Transverse T1-weighted gradient-echo MR images (2D gradient-echo sequence, 290/4.6, and 90° flip angle) and corresponding time course graphs for 45-year-old woman at high genetic risk for breast cancer who underwent screening with dynamic MR imaging. **(a)** In first subtracted postcontrast image for standard dynamic protocol, focal contrast-enhancing lesion (arrow) appeared to have round shape and smooth borders. **(b)** Graph demonstrates type 2 (plateau) signal intensity time course for standard dynamic protocol. Lesion was rated as BI-RADS category 3 (probable fibroadenoma). **(c)** In first subtracted postcontrast image for modified dynamic protocol, lesion (arrow) appeared ill defined and irregular. **(d)** Graph demonstrates type 3 (washout) signal intensity time for modified dynamic protocol. Lesion was rated as BI-RADS category 5. MR-guided excisional biopsy was performed and revealed 6-mm focal high-grade ductal carcinoma in situ.

(second postcontrast images of the standard dynamic protocol and first postcontrast image of the modified dynamic protocol). These findings are in agreement with previously published results on the effect of temporal resolution on use of enhancement rates for differential diagnosis. It is important to note, however, that also for the first postcontrast acquisition of the standard dynamic protocol (ie, 69 seconds after contrast material injection), there was a broad overlap of enhancement rates for benign and malignant lesions, which limited the diagnostic use of this criterion in the individual patient. With a specificity of only 46% and a positive predictive value of 60%, enhancement rates proved to be the weakest of all differential diagostic criteria—even in the first postcontrast image obtained with the standard dynamic protocol.

As opposed to wash-in rates, time course analysis was not affected by the lower temporal resolution brought about by the modified dynamic protocol. In the majority of cases (47 [87%] of 54 lesions), the same time course pattern was assigned with the standard dynamic protocol as was assigned with the modified dynamic protocol. Interestingly, in the seven cases with divergent time course patterns, four appeared to have patterns that were more suspicious with the modified dynamic protocol than with the standard dynamic protocol. Three malignant lesions demonstrated a washout time course with the modified dynamic protocol whereas a plateau time course was demonstrated with the standard dynamic protocol. It was against our expectations to find that the washout time course was identified with the same sensitivity for both dynamic protocols. We had expected that, because of the reduced temporal resolution of the modified dynamic protocol, the dynamic acquisition may not be fast enough to track the rapid signal intensity changes (ie, the rapid upstroke and subsequent loss of signal intensity that constitute a washout time course) that occur in the early and intermediate postcontrast phase. Specifically, we feared that the first postcontrast dynamic images would be obtained too late (ie, only after peak enhancement in the descending part of the signal time course) such that the washout effect would be missed. On the basis of results in 54 enhancing lesions in our study cohort, however, it seems that a sampling rate of just less than 2 minutes was still sufficient to yield the same information on time course pattern as did the standard, 1-minute dynamic series. This was diagnostically important because the differential diagnostic power of this criterion was high, with a sensitivity of 96% (25 of 26 lesions) for both the standard and modified dynamic protocols and a specificity of 86% (24 of 28 lesions) for the standard dynamic protocol and 82% (23 of 28 lesions) for the modified dynamic protocol.

In summary, regarding kinetic analysis, it seems that with the modified dynamic protocol, we do lose the relatively weak diagnostic information provided by enhancement rates, but we do not lose

the relatively powerful diagnostic information provided by time course analysis.

Regarding the second issue—the effect of a moderately increased spatial resolution—our results suggest that the modified dynamic protocol offered substantial and clinically important additional information compared with that afforded by the standard dynamic protocol. Because of the higher anatomic resolution of the modified dynamic protocol, subtle morphologic details of key diagnostic importance that were not visible with the standard dynamic protocol, such as fine spicules or low-signal-intensity internal septations, became apparent. Therefore, readers were able to classify 23 (43%) of 54 lesions more confidently with the modified dynamic protocol than with the standard dynamic protocol. Specifically, nonenhancing internal septations are known to be specific for fibroadenomas (41–43). In seven (29%) of the 24 fibroadenomas, these internal septations were resolved only with the modified dynamic protocol and were not visible with the standard dynamic protocol. Accordingly, these fibroadenomas had been classified as BI-RADS category 3 with the standard dynamic protocol but were correctly downgraded to BI-RADS category 2 with the modified dynamic protocol. The same downgrading was achieved in one intramammary lymph node for which the typical central fatty-tissue signal intensity was identified with the modified dynamic protocol but not with the standard dynamic protocol. This is clinically relevant because a BI-RADS category 2 diagnosis obviates follow-up MR imaging, which is needed to corroborate a BI-RADS category 3 diagnosis. In turn, irregular borders, spicules, or rim enhancement are morphologic features that are known to have a high positive predictive value for breast cancer. These features were visualized only with the modified dynamic protocol in half (13 of 26) of malignant lesions. In nine of 26 malignant lesions, visualization of these features led to a correct upgrading of lesions from BI-RADS category 4 with the standard dynamic protocol to a BI-RADS category 5 with the modified dynamic protocol. Another four malignant lesions were upgraded from a BI-RADS category 3 with the standard dynamic protocol to a BI-RADS category 4 or 5 with the modified dynamic protocol. Aside from aspects of diagnostic confidence, visualization of these features also has an immediate clinical effect because the management of BI-RADS category 3 lesions is usually by follow-up, whereas biopsy is usually recommended for BI-RADS category 4 and 5 lesions.

While the improved visibility of morphologic features proved advantageous for the accurate categorization of 10 benign lesions and 13 malignant lesions, it was, in principle, not advantageous for one patient in whom an enhancing radial scar was present. Here, the improved visibility of spicules led to a false-positive upgrading of one lesion from a BI-RADS category 4 with the standard dynamic protocol to a BI-RADS category 5 with the modified dynamic protocol. We believe, however, that this error is acceptable on clinical grounds—a radial scar is usually considered a high-risk lesion and, owing to the frequent association of radial scars with tubular carcinoma, is treated with local excision.

In summary, with the modified dynamic protocol, lesion morphologic details became detectable, which significantly improved the confidence with which enhancing lesions were classified.

Our study has some limitations that need to be discussed. First, it was not our objective to evaluate whether a higher temporal resolution than that of the standard dynamic protocol would be beneficial for differential diagnosis. We did not investigate this further because, on the basis of previously published material, there is not much reason to suggest that the additional kinetic information obtained by using high-temporal-resolution imaging is superior to the combined analysis of enhancement rates, time course, and morphologic features (32,44). Moreover, it is usually impossible to cover the entire breast parenchyma with these ultrafast pulse sequences. We did not investigate the diagnostic usefulness of pharmacokinetic modeling of our dynamic data and the influence that a reduced temporal resolution (which is a consequence of the modified dynamic protocol) would have had on the pharmacokinetic assessment. Although pharmacokinetic modeling is rarely used in clinical settings, it is conceivable that such modeling may be helpful for further lesion classification. Finally, because all MR images were interpreted by the same two radiologists, it is conceivable that a personal bias was present in that the reader's personal preference regarding the use of morphologic versus kinetic criteria could influence the assignment of BI-RADS categories.

In conclusion, our data suggest that the use of a modified dynamic protocol (ie, a reduced temporal and increased spatial resolution compared with that of the standard dynamic protocol) is associated with a loss of some kinetic information (enhancement rates but not time course patterns). However, because of the broad overlap of enhancement rates of benign and malignant lesions that exists even in the temporally resolved standard dynamic protocol, this diagnostic criterion is of only limited diagnostic value in the individual patient. Kinetic information regarding the analysis of time course patterns is preserved with the modified dynamic protocol and was confirmed to have a high specificity and high positive predictive value. While the kinetic information that was lost with the modified dynamic protocol was of only limited differential diagnostic potency, the morphologic information that was gained was of key diagnostic importance and helped significantly improve our diagnostic confidence regarding classification of enhancing lesions. For this reason, it seems prudent to sacrifice temporal resolution (up to an acquisition time of 2 minutes) in favor of a higher spatial resolution (512 imaging matrix) for dynamic bilateral postcontrast subtracted MR imaging of the breast.

References

1. Baum F, Fischer U, Vosshenrich R, Grabbe E. Classification of hypervascularized lesions in CE MR imaging of the breast. Eur Radiol 2002; 12:1087–1092.
2. Ikeda DM, Hylton NM, Kinkel K, et al. Development, standardization, and testing of a lexicon for reporting contrast-enhanced breast magnetic resonance imaging studies. J Magn Reson Imaging 2001; 13:889–895.
3. Kuhl CK, Mielcarek P, Klaschik S, et al. Are signal time course data useful for differential diagnosis of enhancing lesions in dynamic breast MR imaging? Radiology 1999; 211:101–110.
4. Leong CS, Daniel BL, Herfkens RJ, et al. Characterization of breast lesion morphology with delayed 3DSSMT: an adjunct to dynamic breast MRI. J Magn Reson Imaging 2000; 11:87–96.
5. Liu PF, Debatin JF, Caduff RF, Kacl G, Garzoli E, Krestin GP. Improved diagnostic accuracy in dynamic contrast enhanced MRI of the breast by combined quantitative and qualitative analysis. Br J Radiol 1998; 71(845):501–509.
6. Nunes LW, Schnall MD, Siegelman ES, et al. Diagnostic performance characteristics of architectural features revealed by high spatial-resolution MR imaging of the breast. AJR Am J Roentgenol 1997; 169: 409–415.
7. Schnall MD, Ikeda DM. Lesion diagnosis working group report. J Magn Reson Imaging 1999; 10(6):982–990.
8. Kinkel K, Helbich TH, Esserman LJ, et al. Dynamic high-spatial-resolution MR imaging of suspicious breast lesions: diagnostic criteria and interobserver variability. AJR Am J Roentgenol 2000; 175(1):35–43.

9. Kaiser WA, Zeitler E. MR imaging of the breast: fast imaging sequences with and without Gd-DTPA—preliminary observations. Radiology 1989; 170:681–686.
10. Fischer U, Kopka L, Grabbe E. Breast carcinoma: effect of pre-operative contrast-enhanced MR imaging on the therapeutic approach. Radiology 1999; 213:881–888.
11. Westerhof JP, Fischer U, Moritz JD, Oestmann JW. MR imaging of mammographically detected clustered microcalcifications: is there any value? Radiology 1998; 207:675–681.
12. Kuhl CK, Schmutzler RK, Leutner CC, et al. Breast MR imaging screening in 192 women proved or suspected to be carriers of a breast cancer susceptibility gene: preliminary results. Radiology 2000; 215:267–279.
13. Kuhl CK. MR imaging of breast tumors. Eur Radiol 2000; 10:46–58.
14. Ikeda DM. Progress report from the American College of Radiology Breast MR Imaging Lexicon Committee. Magn Reson Imaging Clin N Am 2001; 9:295–302.
15. Morakkabati N, Leutner CC, Schmiedel A, Schild HH, Kuhl CK. Breast MR imaging during or soon after radiation therapy. Radiology 2003; 229:893–901.
16. DeLong ER, DeLong DM, Clarke-Pearson DL. Comparing the areas under two or more correlated receiver operating characteristic curves: a nonparametric approach. Biometrics 1988; 44:837–845.
17. Bedrosian I, Mick R, Orel SG, et al. Changes in the surgical management of patients with breast carcinoma based on preoperative magnetic resonance imaging. Cancer 2003; 98:468–473.
18. Harms SE. Breast Cancer Staging Working Group report. J Magn Reson Imaging 1999; 10:991–994.
19. Kneeshaw PJ, Turnbull LW, Drew PJ. Role of magnetic resonance imaging in the diagnosis and single-stage surgical resection of invasive lobular carcinoma of the breast. Br J Surg 2002; 89:1296–1301.
20. Liberman L, Morris EA, Kim CM, et al. MR imaging findings in the contralateral breast of women with recently diagnosed breast cancer. AJR Am J Roentgenol 2003; 180:333–341.
21. Liberman L, Morris EA, Dershaw DD, Abramson AF, Tan LK. MR imaging of the ipsilateral breast in women with percutaneously proven breast cancer. AJR Am J Roentgenol 2003; 180:901–910.
22. Lee SG, Orel SG, Woo IJ, et al. MR imaging screening of the contralateral breast in patients with newly diagnosed breast cancer: preliminary results. Radiology 2003; 226: 773–778.
23. Morris EA, Liberman L, Ballon DJ, et al. MRI of occult breast carcinoma in a high-risk population. AJR Am J Roentgenol 2003; 181:619–626.
24. Munot K, Dall B, Achuthan R, Parkin G, Lane S, Horgan K. Role of magnetic resonance imaging in the diagnosis and single-stage surgical resection of invasive lobular carcinoma of the breast. Br J Surg 2002; 89:1296–1301.
25. Orel SG, Schnall MD, Powell M, et al. Staging of suspected breast cancer: effect of MR imaging and MR-guided biopsy. Radiology 1995; 196:115–122.
26. Stoutjesdijk MJ, Boetes C, Jager GJ, et al. Magnetic resonance imaging and mammography in women with a hereditary risk of breast cancer. J Natl Cancer Inst 2001; 93:1095–102.
27. Tilanus-Linthorst MM, Obdeijn IM, Bartels KC, de Koning HJ, Oudkerk M. First experiences in screening women at high risk for breast cancer with MR imaging. Breast Cancer Res Treat 2000; 63:53–60.
28. Warner E, Plewes DB, Shumak RS, et al. Comparison of breast magnetic resonance imaging, mammography, and ultrasound for surveillance of women at high risk for hereditary breast cancer. J Clin Oncol 2001; 19:3524–3531.
29. Hwang ES, Kinkel K, Esserman LJ, Lu Y, Weidner N, Hylton NM. Magnetic resonance imaging in patients diagnosed with ductal carcinoma-in-situ: value in the diagnosis of residual disease, occult invasion, and multicentricity. Ann Surg Oncol 2003; 10:381–388.
30. Agoston AT, Daniel BL, Herfkens RJ, et al. Intensity-modulated parametric mapping for simultaneous display of rapid dynamic and high-spatial-resolution breast MR imaging data. RadioGraphics 2001; 21:217–226.
31. Liberman L, Morris EA, Dershaw DD, Abramson AF, Tan LK. Ductal enhancement on MR imaging of the breast. AJR Am J Roentgenol 2003; 181:519–525.
32. Schorn C, Fischer U, Luftner-Nagel S, Grabbe E. Diagnostic potential of ultrafast contrast-enhanced MRI of the breast in hypervascularized lesions: are there advantages in comparison with standard dynamic MRI? J Comput Assist Tomogr 1999; 23(1):118–122.
33. Boetes C, Barentsz JO, Mus RD, et al. MR characterization of suspicious breast lesions with a gadolinium-enhanced Turbo-FLASH subtraction technique. Radiology 1994; 193:777–781.
34. Hoffmann U, Brix G, Knopp MV, Hess T, Lorenz WJ. Pharmacokinetic mapping of the breast: a new method for dynamic MR mammography. Magn Reson Med 1995; 33:506–514.
35. Knopp MV, Brix G, Junkermann HJ, Sinn HP. MR mammography with pharmacokinetic mapping for monitoring of breast cancer treatment during neoadjuvant therapy. Magn Reson Imaging Clin N Am 1994; 2(4):633–658.
36. Tofts PS, Berkowitz B, Schnall MD. Quantitative analysis of dynamic Gd-DTPA enhancement in breast tumors using a permeability model. Magn Reson Med 1995; 33(4):564–568.
37. Mussurakis S, Gibbs P, Horsman A. Primary breast abnormalities: selective pixel sampling on dynamic gadolinium-enhanced MR images. Radiology 1998; 206: 465–473.
38. Soderstrom CE, Harms SE, Copit DS, et al. Three-dimensional RODEO breast MR imaging of lesions containing ductal carcinoma in situ. Radiology 1996; 201:427–432.
39. Weinstein SP, Orel SG, Heller R, et al. MR imaging of the breast in patients with invasive lobular carcinoma. AJR Am J Roentgenol 2001; 176:399–406.
40. van den Brink JS, Watanabe Y, Kuhl CK, et al. Implications of SENSE MR in routine clinical practice. Eur J Radiol 2003; 46:3–27.
41. Nunes LW, Schnall MD, Orel SG. Update of breast MR imaging architectural interpretation model. Radiology 2001; 219:484–494.
42. Hochman MG, Orel SG, Powell CM, Schnall MD, Reynolds CA, White LN. Fibroadenomas: MR imaging appearances with radiologic-histopathologic correlation. Radiology 1997; 204:123–129.
43. Nunes LW, Schnall MD, Orel SG, et al. Correlation of lesion appearance and histologic findings for the nodes of a breast MR imaging interpretation model. RadioGraphics 1999; 19:79–92.
44. Buckley DL, Mussurakis S, Horsman A. Effect of temporal resolution on the diagnostic efficacy of contrast-enhanced MRI in the conservatively treated breast. J Comput Assist Tomogr 1998; 22:47–51.